PACS numbers: **61.12.–q**, **61.43.–j**, **66.30.–h**
DOI: 10.1070/PU2003v046n11ABEH001672

# Novel approaches to the analysis of crystal structure. A nonstandard method for the study of atomic and molecular diffusion mechanisms

A V Belushkin

## 1. Introduction

Diffraction of X rays and synchrotron radiation is the most widespread method currently in use for the structural analysis of crystals. An important complement to this technique is neutron diffraction. In practical work, powder diffraction is rapidly gaining popularity because new materials are usually synthesized in small amounts insufficient to grow a single crystal. Besides, in certain cases, the growth of a single crystal encounters almost insurmountable difficulties. This has given impetus for the development of new methods to treat powder diffractograms, including those for the elucidation of unknown complex crystal structures (see, for instance, Ref. [1]), not to mention refinement of those structures that were previously described based on the analysis of single crystal diffraction patterns. To make the picture complete, here is a brief description of a procedure for the treatment of powder diffractograms, which is based on the profile analysis first proposed by Rietveld [2]. Because what follows is focused on the studies by the neutron diffraction method, all formulas and discussion below refer to exactly this type of experiment.

In the general case, the experimental histogram for the profile analysis of powder diffraction data is described by the following parametrized function (see, for instance, Ref. [3]):

$$I_i^{\mathrm{c}} = I_i^{\mathrm{bcgr}} + \sum_{m=1}^{N\phi} S_m \sum_{k=k_1}^{k_2} j_{mk} Lp_{mk} O_{mk} |F_{mk}|^2 \Omega_{imk} \,, \qquad (1)$$

where $I_i^{\mathrm{bcgr}}$ is the background intensity for the $i$-th point on the histogram; $S_m$ is the volume fraction of type $m$ phase (for the case of multiphase specimens); $j_k$ is the multiplicity factor for the $k$-th Bragg reflection, i.e., the number of combinations of the Miller indices ($hkl$) corresponding to equal interplanar spacings; $Lp_k$ is the Lorentz factor taking into account the concrete geometry and the type of diffraction experiment; $O_k$ is the factor describing the texture, i.e., deviation from the purely random distribution of relative microcrystal orientations in the sample; $|F_k|$ is the structure factor modulus, including corrections for thermal vibrations of atoms, and $\Omega_{ik}$ is the function describing the shape of diffraction peaks, including the experimental resolution function.

Further data processing is reduced to the minimization of the functional

$$\chi^2 = \sum_i \frac{1}{\sigma_i} (I_i^{\mathrm{expt}} - I_i^{\mathrm{c}})^2 \,, \qquad (2)$$

where $\sigma_i$ is the variance of the $i$-th point on the histogram, and the sum is taken over all experimental points.

The analysis yields a structural model of a crystal that most adequately describes experimental data, based on appropriate criteria. As pointed out above, current methods for the analysis of powder diffractograms, including the briefly described profile analysis, permit us to study rather complex ordered crystal structures. However, traditional methods of data analysis take into account neither static nor dynamic disorder in crystals, setting aside a large number of related methodical and mathematical problems that are beyond the scope of the present paper. The matter is that the disorder effects contribute to background intensity $I_i^{\mathrm{bcgr}}$ of function (1) which in standard approaches is approximated by a polynomial or other smooth function. By way of example, Fig. 1 shows the neutron diffraction spectrum of a $CsDSO_4$ sample in the high ionic conduction phase. The diffraction pattern is indicative of modulated substructure caused by diffuse neutron scattering from deuterons diffusing through the sample. Other data processing methods are needed to derive physically significant information from this diffuse scattering. One of the approaches extensively employed for solving these problems in recent years is inverse Monte Carlo simulation.

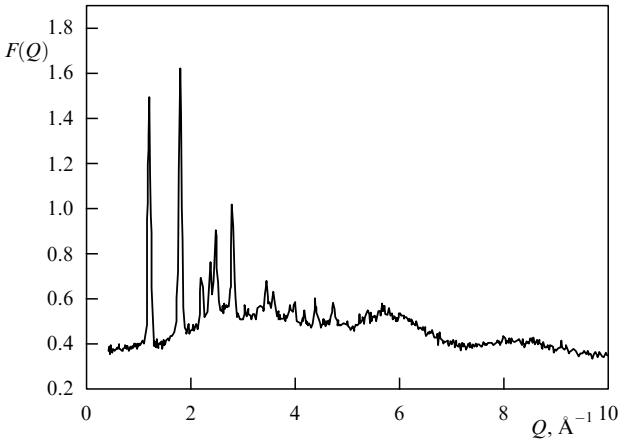


**Figure 1.** Neutron diffraction spectrum of a $CsDSO_4$ sample for the high protonic conduction phase. Notice modulated diffuse scattering due to proton motions in the specimen.

## 2. Inverse Monte Carlo method

In inverse Monte Carlo modeling, the structure of the object of interest is described by means of a pair radial correlation function defined as

$$g(r) = \frac{n(r)\,\mathrm{d}r}{4\pi n_0 r^2\,\mathrm{d}r} \,. \qquad (3)$$

Here, $n_0$ is the average atomic number density in a substance, and $n(r)\,\mathrm{d}r$ is the number of atoms in the spherical layer of radius $r$ and thickness $\mathrm{d}r$ that encloses an atom arbitrarily selected as the origin of the coordinates.

A diffraction experiment allows us to measure (after taking into account necessary calibrations and corrections) the Fourier transform of the correlation function $g(r)$:

$$F^{\mathrm{expt}}(Q) = \frac{4\pi n_0}{Q} \int_0^{+\infty} r\, g(r) \sin(Qr)\,\mathrm{d}r \,, \qquad (4)$$

referred to as the total structure factor. Here, $Q$ is the modulus of the neutron momentum transfer during the process of scattering.

Without going into details, the data treatment procedure using the inverse Monte Carlo method can be described as

follows. First, a structural model is constructed, based, as a rule, on the previously obtained data or well-grounded propositions concerning the object of interest. The pair radial correlation function and the corresponding total structure factor $F_0^{\text{calc}}(Q)$ are calculated for the model. Second, the calculated and measured structure factors are compared, based on the maximum likelihood criterion:

$$\chi_0^2 = \frac{\sum_i \left[F_0^{\text{calc}}(Q_i) - F^{\text{expt}}(Q_i)\right]^2}{\sigma^2(Q_i)}\,, \tag{5}$$

where the sum is taken over all points of the experimental spectrum, included in the data analysis. Here, $\sigma(Q_i)$ is the variance of the $i$-th point of the experimental profile. Thereafter, an arbitrarily selected atom is displaced in a random manner in any direction. For the newly obtained structural model, a new correlation function $g_n(r)$, total structure factor $F_n^{\text{calc}}(Q)$, and corresponding maximum likelihood parameter $\chi_n^2$ are computed. If $\chi_n^2$ is found to be smaller than the parameter calculated for the previous configuration, then the new structural model is accepted with probability $w = \exp[-(\chi_n^2 - \chi_{n-1}^2)/2]$ and is rejected otherwise.

As a result, the parameter $\chi_n^2$ reduces in the course of data analysis to a certain minimal value corresponding to the structural model of the object under study, which is within the limits of experimental accuracy being consistent with the available measurement data. This algorithm realizes the so-called 'Markovian process', therefore the resultant structural model proves to be statistically independent of the initially chosen three-dimensional atomic configuration.

A major advantage of inverse Monte Carlo simulation is its applicability to the structural analysis of highly disordered systems, such as liquids and glasses, that are impossible to study using the conventional profile analysis described in the preceding section. Moreover, this approach (unlike, for example, the molecular dynamics method) makes unnecessary any assumption about a character of interatomic interactions.

Naturally, the inverse Monte Carlo technique (like any other method for the analysis of experimental data) has proper constraints. Readers are referred to Ref. [4] and other articles in the same issue of the journal *Nuclear Instruments and Methods* for more information about merits and demerits of the method under consideration.

## 3. Application of inverse Monte Carlo simulation to the analysis of rotational and translational diffusion in crystals

### 3.1 Superprotonic conductor $CsHSO_4$

Cesium hydrosulfate ($CsHSO_4$) was the first compound of the $MXAO_4$ family ($M$ = Cs, Rb, $NH_4$; $X$ = H, D; $A$ = S, Se) in which transition to the state with superprotonic conduction was observed. The crystal did not melt during this process but underwent instead first-order phase transition at $T_c = 414$ K, leading to a 4 orders-of-magnitude increase in conductivity that eventually amounted to $10^{-2}\ \Omega^{-1}\ \text{cm}^{-1}$ [5]. Changes in the structure of $CsHSO_4$ crystals during the phase transition of interest were measured by X-ray diffraction experiments on single crystals and powders and by powder neutron diffraction. For a rather long time the literature contained conflicting data. The discrepancy was attributable to the fact that the phase transition is a ferroelastic phase transition characterized by strong spontaneous deformation ($10^{-2}$) which causes the deterioration of large single crystals. An additional difficulty in structural interpretation of the superprotonic phase is related to the high degree of its disorder. Today, the microscopic mechanism of phase transition to a state with high protonic conduction, the proton diffusion mechanism, and other physical properties of crystals of this new family are known fairly well (see, for instance, the review article [6]).

The most reliable structural information was obtained in powder neutron diffraction experiments using deuterated samples [7]. It was demonstrated that, below the transition temperature to the superprotonic state, a crystal has a monoclinic unit cell (space group $P2_1/c$), while the superprotonic phase is tetragonal (space group $I4_1/amd$). In the monoclinic phase, hydrogen bonds link $SO_4$ tetrahedra so as to form zigzag chains. Orientation of each tetrahedron is well-determined, and the deuterons are localized on hydrogen bonds. Other potential sites of deuterons in the structure are energetically disadvantageous. These conclusions are based on the small values of thermal parameters of atoms in the structure and logically related to low protonic conduction in the given phase.

In the superprotonic phase, $SO_4$ tetrahedra occupy four different orientations and are therefore disordered. Owing to this disorder, a crystal cell contains six energetically equivalent positions per proton (instead of one as in the low-conducting phase). As a result, migration of protons between these sites effect the high protonic conduction. The four possible orientations of a tetrahedron also suggest that the configurational entropy of the phase transition must be $R\ln 4 \approx 1.39$, i.e., close to the experimentally found value.

The diffusion of protons in the superprotonic phase of $CsHSO_4$ was investigated in detail by incoherent quasi-elastic neutron scattering method [8]. The data obtained were analyzed taking into consideration the known structural peculiarities of the material under study and used to postulate the two-step proton diffusion mechanism described below. At the first stage, a proton displaces towards one of the two $SO_4$ groups that form a hydrogen bond. The displacement causes a defect, viz. $HSO_4^-$. At the second stage, the longer (hence, weaker) half of the hydrogen bond is broken, and the $HSO_4^-$ group is rotated to occupy a new position. The reorientation of the defects continues till a new hydrogen bond with the neighboring sulfate group is formed. Thereafter, the process is repeated, resulting in translational diffusion of protons through the crystal lattice. Thus, the specimen undergoes a relatively rapid rotational diffusion of $HSO_4^-$ defects and a slower translational diffusion of protons. The mechanism is illustrated schematically in Fig. 2, showing one of the possible paths of proton transport.

The proton diffusion mechanism proposed and quantitative characteristics of the process, obtained in the neutron scattering study, are in excellent agreement with the results of other experiments carried out with the use of calorimetry, optical spectroscopy, and NMR method. However, because the profile analysis of diffraction data only yields information about the most likely average positions of atoms in a crystal and because the interpretation of the results of quasi-elastic neutron scattering is based on model assumptions, it seems appropriate to validate the above conclusions by an independent method. Such a possibility is provided by inverse Monte Carlo modeling.

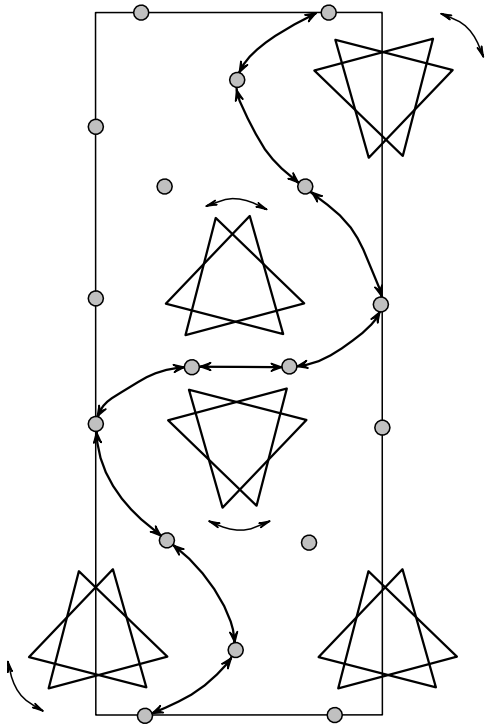

**Figure 2.** Schematic representation of the proton diffusion mechanism in the superprotonic phase of $CsHSO_4$. The figure portrays two of the four possible orientations of $SO_4$ tetrahedra and one of the many conceivable paths of protons transferred through the crystal lattice. Circles and squares mark possible proton positions deduced from the results of powder neutron diffraction experiments.

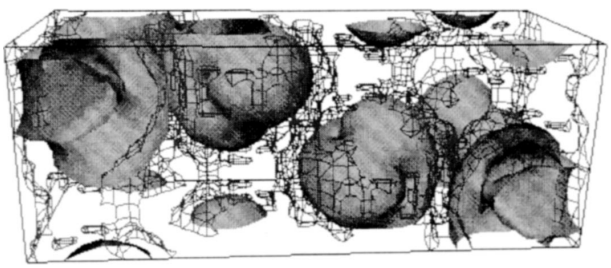

**Figure 3.** Atomic density distribution in a unit cell of the $CsDSO_4$ superprotonic phase, as deduced from data analysis by the inverse Monte Carlo technique. Distorted spherical shells correspond to $SO_4$ groups, and the grid of lines to deuterium density distribution. Cesium atoms are not shown.

Figure 3 shows atomic density distribution in a $CsDSO_4$ unit cell in the superprotonic phase, deduced from the analysis of neutron diffraction data by the inverse Monte Carlo technique [9, 10]. It can be seen that the atomic density distributions of sulfate groups and deuterium do not overlap. Nor is there a superposition of density distributions of the sulfate groups and cesium atoms. The patterns of atomic density distribution of sulfate groups confirm information about their rotational diffusion in the superprotonic phase. The observed distortion of the spherical shape of the distribution is fully consistent with the most probable orientational states of $SO_4$ tetrahedra, identified based on the results of the profile analysis of the diffraction spectra. An in-depth deuterium density distribution study not only allowed us to visualize the most likely proton transfer channels but also confirmed the strong correlation between proton transfer and the rotation of sulfate groups. Moreover, a number of important questions concerning pretransitional phenomena in the specimen were clarified.

Thus, a combination of different neutron scattering techniques and modern data processing methods made it possible to draw an unambiguous picture of phase transition to the state with superprotonic conduction and elucidate the microscopic mechanism of proton transfer throughout the crystal lattice.

### 3.2. Ammonium chloride $NH_4Cl$

Ammonium chloride, $ND_4Cl$ ($NH_4Cl$), provides a convenient model for theoretical analysis of order–disorder phase transitions in molecular–ionic and molecular crystals. A variety of phenomena associated with this compound and characteristic of many other molecular and molecular–ionic crystals have long been researchers' focus of attention. A unit cell of the ammonium chloride structure at room temperature has a cubic form with $Cl^-$ ions at the vertices, and a molecular ion $ND_4^+$ in the center. Because there are two energetically equivalent positions per ammonium ion, the ammonium ions randomly occupy one of them. In the course of time, $ND_4^+$ ions can execute jumps (reorientations) from one equivalent position to the other, which leads to dynamic orientational disorder.

An ammonium ion has a shape of a tetrahedron, and the transition from one equivalent position to the other can be described as jump reorientation of the ion at an angle of 90° with respect to one of its axes of symmetry passing through the midpoints of two opposite edges of the tetrahedron, which are orthogonal to each other. In addition, an ammonium ion may undergo reorientations at an angle of 120° with respect to other types of symmetry axes passing through the vertices and the centers of opposite bases of the tetrahedron; such reorientations do not change the ion position.

Analysis of the geometry of orientational disorder in $ND_4Cl$ permits us to identify the predominant type of ion reorientations [11]. Inverse Monte Carlo simulation of the $ND_4Cl$ neutron diffraction spectrum yielded the spatial density distribution of deuterium atoms in a unit cell (Fig. 4). The atoms turned out to be arranged in a cubic structure, in agreement with the distribution symmetry of the nearest halogen ions about the ammonium ion. The centers of density distribution at the vertices of the cube correspond to the equilibrium positions of deuterium atoms for two equivalent orientations of $ND_4^+$ ions in the structure. The density distribution of D atoms at the vertices of the cube reflects libration vibrations of $ND_4^+$ ions (angular vibrations of ions as a whole about equilibrium position). The density distribution of D atoms along the edges of a cube that connect its vertices corresponds to the reorientations of ammonium ions between the two equivalent positions by executing jump rotations through 90°.

Another possible type of reorientations, viz. rotation of ammonium ions (by 120°) not resulting in the ion jumps from one position to the other, must correspond to the density distribution of D atoms along the diagonals of the cube faces. However, such distribution contradicts to the obtained result. Its contribution is estimated at no more than 5%.

The geometric pattern of dynamic orientational disorder in $ND_4Cl$, revealed with the aid of inverse Monte Carlo modeling, is consistent with the results of analysis of

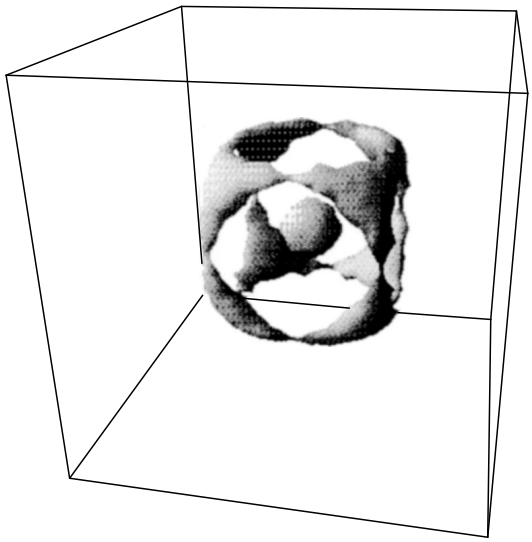

**Figure 4.** Averaged spatial distribution of deuterium density in a unit cell of $ND_4Cl$.

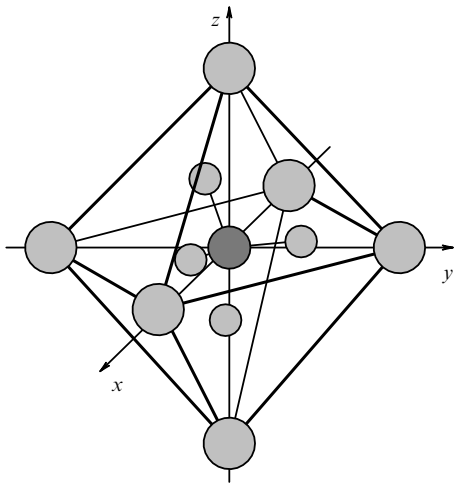


**Figure 5.** The octahedral environment of an ammonium ion in $ND_4I$ structure. The figure shows one of the possible positions of $ND_4^+$ for the structural model in which three of the four N – D...I bonds have equal lengths.

orientational disorder in ammonium ions constituting the related compound $NH_4Br$ with an identical structure; these results were obtained by quasi-elastic neutron scattering spectroscopy [12]. This observation provides one more argument supporting the validity of findings described in preceding paragraphs.

### 3.3 Ammonium iodide $ND_4I$

Ammonium iodide, $ND_4I$ ($NH_4I$), exemplifies a more complex case of orientational disorder in ammonium ions compared with ammonium chloride. A unit cell of the ammonium iodide structure at room temperature also has a cubic form, with $I^-$ ions occupying vertices and face midpoints and $ND_4I$ ions located in the center of the cube itself and its edges. In the literature, such a structure is frequently referred to as that of the common salt (NaCl) type. Here, the nearest iodine ions make up an octahedron that encloses a tetrahedral $ND_4^+$ ion at its center. Such a configuration hampers simultaneous approaching of all four N – D bonds of ammonium ions to the six iodine ions to attain the minimally possible distances between them and form four equipollent hydrogen bonds N – D...I as in $ND_4Cl$, hence, a higher degree of ion disorder in $ND_4I$, akin to that in free rotation.

The equilibrium crystal structure of $ND_4I$ can be described using several models with a different number of equally long N – D...I bonds. The model with the least possible number of equivalent positions for ammonium ions (eight) possesses the highest symmetry degree. In this model, three of the four N – D...I bonds are of equal length and make an angle to coordinate axes $x$, $y$, and $z$, which is somewhat different from 180°; the fourth N – D bond is aligned parallel to the spatial diagonal of the cube [13] (Fig. 5).

Traditional methods of structural analysis appear to be of little value for assessing the validity of possible models of $ND_4I$ structure. The assessment needs to be supplemented by the analysis of the geometry of orientational disorder in ammonium ions that governs the spatial distribution of deuterium atoms in the structure. Such analysis was made using inverse Monte Carlo simulation. The result of modeling deuterium density distribution over the unit cell is shown in Fig. 6.

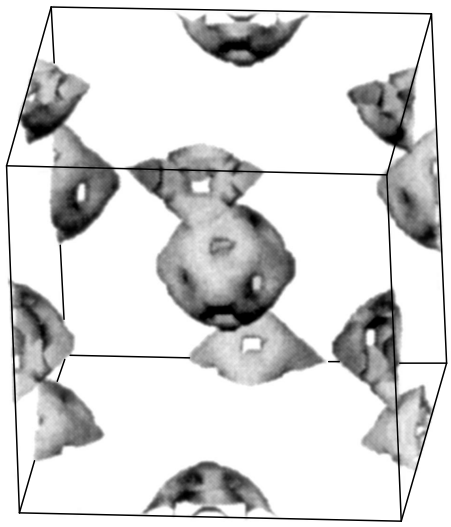

**Figure 6.** Averaged spatial distribution of deuterium density in a unit cell of $ND_4I$.

Deuterium atoms are arranged in the form of an octahedron, which reflects the local symmetry of the nearest halogen ions surrounding an ammonium ion. This picture is consistent with the above structural model with eight equivalent sites for ammonium ions. N – D bonds oriented in the vicinity of axes $x$, $y$, and $z$ determine the density distribution of deuterium atoms in the form of squares, while N – D bonds oriented along spatial diagonals of the cube are responsible for spherical distributions broadened by virtue of libration of ammonium ions. The presence of the region of overlap for these distributions indicates that reorientations of ammonium ions in $ND_4I$ occur as a result of jump rotations of N – D bonds from positions oriented parallel to the spatial diagonals of the cube to positions in the vicinity of axes $x$, $y$, and $z$.

Such geometric pattern of orientational disorder of ammonium ions in $ND_4I$ agrees with the results of an earlier study on the dynamic characteristics of orientational disorder in ammonium iodide, performed with the use of quasi-elastic

neutron scattering spectroscopy [14]. This study has demonstrated that the available experimental data can be rationally interpreted only on the assumption that ammonium ions undergo jump rotations through the angles less than 90°. However, it proved impossible to accurately determine the angle and construct a geometric model of orientational disorder in ammonium iodide, based on dynamic characteristics.

The above examples for the structure of disordered phases in ammonium halides allow for the conclusion that the disparity between the local symmetry of a molecule and the symmetry of its local environment in a crystal can be removed by dynamic orientational disordering in which the symmetry of atomic density distribution in a molecule matches that of the environment.

## 4. Conclusion

A combination of standard methods (e.g., the Rietveld method) and nontraditional structural analysis, such as inverse Monte Carlo simulation, opens bright prospects for the investigation of complex crystal systems with a dynamic disorder of individual molecular groups or atoms. Standard methods are used to construct a structural model of an ordered crystal 'core' and determine the most probable positions of disordered molecular groups and atoms. Thereafter, the inverse Monte Carlo technique is employed to determine the geometric pattern of orientational disorder in the molecules and diffusion paths of atoms in the crystal along with characteristic geometric parameters of diffusion processes in comparison with the data obtained by other experimental methods.

The author wishes to acknowledge gratefully collaboration with R L McGreevy, P Zetterstrom, and D P Kozlenko in the course of this joint study. Thanks are also due to the administrations of the ISIS neutron source at the Rutherford-Appleton Laboratory, UK, and the NFL Neutron Laboratory at Studsvik, Sweden, for the possibility of carrying out experiments using their facilities.

## References

1. Wessels T et al. *J. Am. Chem. Soc.* **121** 6242 (1999)
2. Rietveld H M *J. Appl. Cryst.* **2** 65 (1969)
3. Aksenov V L, Balagurov A M *Usp. Fiz. Nauk* **166** 955 (1996) [*Phys. Usp.* **39** 897 (1996)]
4. McGreevy R L *Nucl. Instrum. Meth. A* **354** 1 (1995)
5. Baranov A I, Shuvalov L A, Shchagina N M *Pis'ma Zh. Eksp. Teor. Fiz.* **36** 381 (1982) [*JETP Lett.* **36** 459 (1982)]
6. Belushkin A V *Kristallografiya* **42** 549 (1997) [*Crystallogr. Rep.* **42** 501 (1997)]
7. Belushkin A V et al. *Acta Cryst. B* **47** 161 (1991)
8. Belushkin A V, Carlile C J, Shuvalov L A *J. Phys.: Condens. Matter* **4** 389 (1992)
9. Zetterström P et al. *Solid State Ionics* **116** 321 (1999)
10. Belushkin A V *Solid State Ionics* **125** 61 (1999)
11. Belushkin A V et al. *Physica B* **269** 297 (1999)
12. Lechner R E et al. *J. Chem. Phys.* **73** 934 (1980)
13. Paasch M et al. *Z. Phys. B: Cond. Mat.* **99** 339 (1996)
14. Goyal P S, Dasannacharya B A *J. Phys. C: Solid State Phys.* **12** 219 (1979)